NASA TECHNICAL MEMORANDUM

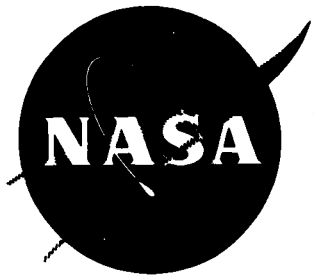


NASA TM X-52169

NASA TM X-52169



# STATIC LOAD TESTS ON RESEARCH AND DEVELOPMENT ATLAS VEHICLE LAUNCHER

by Holmes Neal
Lewis Research Center
Cleveland, Ohio



NATIONAL AERONAUTICS AND SPACE ADMINISTRATION · WASHINGTON, D.C. · 1966

# STATIC LOAD TESTS ON RESEARCH AND DEVELOPMENT ATLAS VEHICLE LAUNCHER

by Holmes Neal

Lewis Research Center
Cleveland, Ohio

NATIONAL AERONAUTICS AND SPACE ADMINISTRATION

# STATIC LOAD TESTS ON RESEARCH AND DEVELOPMENT ATLAS VEHICLE LAUNCHER

by Holmes Neal

Lewis Research Center
National Aeronautics and Space Administration
Cleveland, Ohio

E-3325

## SUMMARY

A series of static loads were applied to one end frame and one balance longeron of the launcher, and fifty cycles of alternately applied loads were made to both end frames. The first category of loads was used to check stresses and design, whereas the second was used to study the effect of repetitive loading on cracks that were known to exist. Most of the weld areas had acceptable stress levels. Small areas with local high stresses could be greatly improved with a minor amount of rework on some details with one exception; the welds that secure the holddown release cylinder blocks to the end frame are highly stressed to the point of yield. The overall design is adequate, and member sizes are satisfactory. The cyclic loading did not produce any discernible deleterious effects.

## INTRODUCTION

In the spring of 1963, it became evident that some means should be developed to evaluate the structural adequacy of the research and development launchers used in the Atlas-Centaur program. These launchers were designed, developed, and fabricated at the beginning of the research and development phase of the Atlas program, but they were not designed for a long-range operating program. Quality-control practices for welding were lax. The results of a survey indicated that several cracks existed in the weld areas. It was also noted that these cracks were present in no particular pattern but were randomly located.

The launcher, as used in the Atlas-Centaur program, must support more gravity load and have more wind-exposure area to cause greater overturning moment than that for which it was designed. These effects combined to restrict ground winds at launch time to such a low value as to endanger conceivably the launch probability for short-time windows. The testing method should be adaptable to operational launchers and thus obviate the need for removal of the launcher from the site, which minimizes cost and loss of time. The data gathered from the static load test in conjunction with information from a separate test, which monitors moment as a function of wind, should provide justification for improving this launch condition. A launcher was assembled at Lewis Research Center for the test, utilizing a load-fixture design that had been made for the U. S. Air Force.

## DESCRIPTION OF LAUNCHER

Structurally speaking, the launcher could be thought of as an adapter that provides a means of supporting and transferring vehicular loads to the concrete foundation. The launcher used in this test was an Atlas research and development type, as shown in figure 1. The main rectangular frame, composed of two U-shaped and two tubular center supports (spool pieces), has a tripod frame mounted on each corner. A pair of these tripod frames, on each end of the main frame (hereinafter referred to as an end frame), forms a stanchion at each end, on which each arm of the support arm and mechanism assembly is mounted. All these components are fabricated of heavy wall low-carbon steel pipe and plate. The support plate and mechanism assemblies consist of two wishbone shaped housings constructed of heavy welded steel plate. Missile holddown pin and pin-actuating mechanisms are contained in each of these housings. A holddown and release cylinder connects the bottom of each support arm and mechanism assembly to the middle of the tripods of each U-shaped structure. The cylinders are pressurized to stabilize the missile but are vented at launch.

A hinged auxiliary support is mounted on each side of the main rectangular frame that serves to balance the erected missile. Each auxiliary support consists of a tripod, a vertical support pin, and an actuating cylinder. The vertical support pins are mounted at the apexes of the auxiliary supports and are interconnected and pressurized to provide the missile-stabilizing system. At launch, these auxiliary supports are pneumatically pivoted outward to clear the rising vehicle.

## PURPOSE OF TEST

Tests were conducted on this launcher to establish a level of confidence in its structural function. Special attention was given to the following areas:

(1) Behavior of the existing cracks in the test article

(2) Stress measurements in certain areas corresponding with load application

(3) Need for and the practicability of devising a method to reinforce weak points of the structural frame

## TESTS AND APPLICATION DEFINED

The philosophy adopted in these tests has been that of a gross approach rather than that of precise procedures and exact values. Thus, information of a general nature should be sought and areas of variation, which are inherent in these launcher structures, avoided. Therefore, it was deemed admissible that the test (always vertical) loads should not

simulate operating loads exactly, that data should not be corrected for every known variance, and that conclusions could be made that would be of a more general nature and thereby have more applicability.

### Proof Loading One End Frame (Quadrants I and IV)

A photoelastic coating material was applied to the major load-carrying weld areas in quadrant I (see table I). Twelve strain gages were applied to certain members in this quadrant, as shown in figure 2.

### Proof Loading One Auxiliary Frame (Quadrants III and IV)

A photoelastic coating material was applied to the critical load-carrying welds on the balance longeron frame (fig. 17). Strain gages were not used on this part of the structure. The frame had only one load applied, namely 128 kips.

### Cyclic Loading of Each End Frame

The same photoelastic coating material referred to in the preceding test was used in this test in a visual-qualitative sense (table II) by using polarized light to determine whether existing cracks grew or if new ones appeared. Strain gages were not used. When the test was run on the opposite end frame (quadrants II and III), dye-penetrant applications were made before and after the load applications.

### Material Properties

Small areas of base and weld metal were ground and polished so that hardness tests could be made to evaluate some material properties.

## TEST PREPARATIONS

The launcher was assembled and supported on heavy timber blocking located as close as possible to the launcher z-axis supports. Only one holddown head was installed using a static link to support it. The test fixture was attached to the launcher frame by using the z-axis support rings. The source of loading for these tests was a 300-ton double-acting hydraulic cylinder. A special adapter (fig. 7) was made to engage the loading cylinder piston rod with the vehicle holddown pin. The base of the load cylinder was fastened to the top of the test fixture, as shown in figures 7 and 8.

Scales were arranged to measure the change in the horizontal distances between centerlines of the 20-inch-diameter pipe and in the vertical distances between the horizontal centerline of the 20-inch-diameter pipe and the main support pin. These readings were made before and after the release of every load to check on any general yielding condition. (See fig. 9 for typical arrangement.)

Two loading fixtures were used in this test, one at either end of the launcher. An additional frame, like an inverted U, was fastened to the top of the two loading fixtures located vertically over the balance longeron pins to apply load to the longeron frames, as shown in figure 10. The hydraulic jack was then mounted on the bottom side of the overhead beam. A special adapter was used to transmit the downward load only to the pin. The balance longeron pins are normally supported by a hydraulic-pneumatic system, which was not used in this test. Instead, a static link was used for support. The load applied to the pin in this test did not prove the hydraulic-pneumatic system, rather it was a structural test for the longeron frame.

One of the purposes of this program was to ascertain some knowledge of the load-stress relation because design calculations were not available. To pursue this aim within the level of accuracy as previously defined, twelve strain gages were installed, in pairs of two, in six areas on the members in quadrant I. All the gages were installed on parent metal and at sufficient distance from connections to be free of local and discontinuity stresses. Each gage of each pair was located diametrically opposite the other and at the same station. Each was oriented to measure strain parallel with the members, data collected from each pair could be converted into total direct load and bending moment for the member. The diameter on which the gages were located was chosen arbitrarily to a degree, but by using judgement and knowledge of the anticipated bending action of the applied loads, it is believed that the plane of maximum moment was quite closely ascertained.

A tent was set up over quadrants I and IV of the launcher to minimize temperature changes that might be caused by climatic conditions during any particular test. A photoelastic coating was used to facilitate the evaluation of stresses, and even yield, in the weld areas due to the applied loads. Prior to coating, all areas were sandblasted to remove paint and other foreign materials. The coating was applied by the surface forming technique described in the appendix.

The major load-carrying welds in quadrants II and III were sandblasted in preparation for dye-penetrant inspection for the load cycle tests. The dye penetrant was not used in quadrants I and IV for the load cycle test, but cracks that were known to exist from prior inspection were identified by prick-punch marks before the loading began. After the application of a series of cyclic loads, the cracks were examined for growth by a dye-penetrant inspection conducted in accordance with MIL-I-6866. The photographs in figure 11 show typical areas before and after testing for the purpose of comparison.

Small spots in the weld and parent metal areas were ground and polished so that BHN could be obtained. A portable Telebrineller was used to secure these data. Figure 12 shows the test locations on the launcher and the resulting ultimate tensile stresses at the corresponding points.

## TEST RESULTS

### Proof Loading One End Frame

Table III presents the reduction of the stress data indicated by the strain gages in the proof loading tests. The applied loads ranged from 20 kips less than the maximum normal anticipated vehicle load to 1.5 times greater, with abort conditions neglected. The data are plotted in figure 13. An examination of the curves shows that none of the strain gages recorded a yield stress, and only one located a stress above the normally accepted design value. None of the curves has a uniform stress-load relation, which indicates that the structure is not a so-called simple structure, but a redundant structure. All the gages except four showed a decreasing slope with increasing load, indicating that, with increasing load and deflection, other members are participating in reacting the load as these four curves appear to do. The stress measured by these four gages was low for the applied loads. The slope is such at the high-load end as to indicate that acceptable stress values will prevail for any reasonable load application. This phenomenon should mean that the structure will support more load than the design specifies, if good joints are assumed.

Table I presents data gathered from the photoelastic coating in the proof loading tests on one end frame. The location of the points shown in the table may be found by the following method:

Area 1: position 3 is designated as point 13.

Area 6: position 11 is designated as point 6-11.

The average thickness of all photoelastic sheets was 0.105 inch after forming and setting, with a variation of ±0.005 inch. Taking into account the strain-optical sensitivity of PL-1 plastic, K = 0.10, gives the fringe value f (difference of principal strains affecting one fringe):

$$F = \frac{11.35}{tK}$$

$$= 1080 \quad \mu\text{in./in./fringe}$$

The sensitivity of measurement of the analyzer is 1/30 to 1/50 of a fringe in field testing. Measurements on plastic, f = 1080, could therefore yield a strain sensitivity of ±30 micron inches per inch. At every load, measurements of stresses were made at significant points. After unloading, the areas were observed to detect residual deformation. Figures 14 to 17 illustrate the coating application and show the location of points.

General observations of the photoelastic coating during the load applications and an examination of the recorded data are as follows (unless otherwise noted the direction of principal stress is perpendicular to weld line):

Area 1. - The maximum stress level was noted at point 14 in the fillet by the weld. The gradient was very high, and within a distance of 1/2 inch, the stress decayed to one-third of the maximum stress. The stress in weld is smaller on the front than on the back, and the gradient is flatter.

Area 2. - The stress level in this area remained low for all loads.

Area 3. - Only three points in this area indicated a high stress level; points 31, 33, and 34. The highest stress was observed at point 33, where the apex of the M-shaped plate is welded to the vertical tubular member. The remainder of this area (point 35) and the similar area on the back exhibited a very low stress level.

Area 4. - The stress on the front was low except at the end of the weld where a local concentration was observed. The stress on the back was high and uniform from point 47 to 46 and then decreased rapidly.

Area 5. - The stress in this area did not exceed 25 000 pounds per square inch for the largest load.

Area 6. - Unlike any other areas, stresses were high in all welds that were more or less parallel with the diagonal tubular member above it. A stress concentration was observed at point 6-11 as a result of the stiffening effect and discontinuity of a pad welded to the horizontal tubular member.

Area 7. - The maximum stress was measured at a point located approximately in the plane of symmetry of the intersection, and the direction of the principal stress was $40^{\circ}$ to the vertical plane.

Area 8. - Two points of high stress were noted, similar to area 3 on the front. Point 82 is in the weld at the apex of the M-shaped plate that secures it to the vertical tabular member. Point 81 appears to be the most critical of all areas analyzed. High residual deformation was observed at this point even for reversed loads; this deformation was first observed for the 186-kip load.

Note that unless otherwise stated, the principal stresses were always perpendicular to the weld line. Points 43, 47, 61, 65, 67, 6-10, and 81 are located on edges so that the difference of principal stresses is equal to the maximum stress tangent to the edge.

## Proof Loading One Auxiliary Frame

One 128-kip down load was applied to the balance longeron frame to check its structural integrity. Photoelastic material was applied to the joint area at the apex of the frame. A cursory analysis of the auxiliary frame indicated the critical area (structurally speaking) to be in the vicinity where the auxiliary pin load is transmitted to the strucural frame, bearing values, welds in shear, etc.

Some yielding was detected in the plates below the pin that engages the lower end of the auxiliary pneumatic balance cylinder. This is a bearing stress, and the instability of the area is not a consideration. Because the test load was 170 percent greater than present requirements and 33 percent greater than any contemplated load, this does not have any particular significance. Again, the x-direction is perpendicular to the weld. To obtain the difference of principal stresses $\sigma_x - \sigma_y$, multiply the difference in principal strains $\epsilon_x - \epsilon_y$ by $\epsilon/(1 + \mu) = 23 \times 10^6$. Since the strains are expressed in $10^{-6}$ $\mu$-inch per inch, it is sufficient to multiply the numbers in the table by 23, that is, for those in the elastic range.

## Cyclic Loading of Each End Frame

During the first cycling test, the stress patterns in the photoelastic coating material were continually observed to discern any change. There was no change. This material was known to cover two original cracks. Stress patterns were evident about the cracks, but for the entire test, the change in this pattern was imperceptible. The loads applied to the second end frame were about 10 percent greater than those in the first cycle test. These loads were increased because of the favorable results of the first test. This appeared to be a safe increase relative to the strength of the launcher, yet greater than the normal operating loads, thereby raising the level of confidence in the launcher if the outcome of the second test was favorable. The ends of two cracks, about 4 inches long and readily seen with the naked eye, were prick-punched before the test began. The ends were determined by the dye penetrant. Any growth that may have occurred during the loadings was not discernible by this method.

## Material Properties

The points for this test were selected at random. No effort was made to obtain comparative data in the parent metal and adjacent weld metal, but to discern if the effect of work hardening could be observed. This test was the last in the sequence, that is, after all loading was completed. The values in figure 11 appear fairly consistent, but are generally higher than expected; however, this is not necessarily an indication of strain hardening because it is known that some of the points (e.g., 411 and 911) are in low-stress areas.

Specification values: all pipe material is ASTM-A53-47, Grd. B; the ultimate stress is 60 ksi, and the tensile yield stress is 35 ksi. All plate material is AISI 1010 or 1020, the ultimate stress is 55 ksi, the tensile yield stress is 36 ksi, and the ultimate bearing stress is 90 ksi. The weld design allowables for ASTM materials are tensile stress, 32.2 ksi, and shearing stress, 20.2 ksi (ref. 1). The weld design allowables for AISI 1010-1020 steels are tensile stress, 18.4 ksi, and shearing stress, 11.5 psi (ref. 1).

## DISCUSSION OF RESULTS

It is apparent that this series of loads indicated that the launcher design is adequate; however, it is recognized that this loading does not completely simulate loads of every design condition. When the effect of these unaccounted for loads is compared with that of the applied loads, the resulting maximum stress is never significantly increased because

(1) The unaccounted for loads are comparatively small

(2) The stresses resulting therefrom are not always additive

(3) The location of the maximum stresses resulting from the unaccounted for loads seldom, if ever, corresponds with the location of maximum stresses for the applied loads

The foregoing conclusions have been reached, however, contingent on a decision not to consider an "abort" as a worthy loading condition because of its improbable occurrence. This series of loads did produce high stresses, in fact yielding in some parts of the welds. The high stresses and yielding were of a localized nature, with only one exception that will be treated later in this report. Only a small portion of a total joint weld, about 5 to 10 percent, would be highly stressed or even yielding. The remaining portion would not indicate any distress at all. The photoelastic material indicated this stress variation very well. These stress concentrations are caused by several conditions, namely,

(1) Welds have to work (i.e., carry load) in a disadvantageous manner (root opening too large)

(2) Sharp acute angles at the joint between parts of one member and parts of another member

(3) Relation of load-carrying capability features of the structural members as they meet at a joint, that is, if rigid (high-load-carrying ability) portions of one member mate at a joint with similar features in another member, a region of high stress occurs

The provisions that were made to indicate changes in two major dimensions on the launcher (see fig. 9) did not reveal any readable changes. It is therefore concluded that the loading did not cause any member failure or general yielding.

Good welds in the structure do not need modification or redesign for the present launch conditions; however, the launcher load-carrying capability will be improved by and in the order of each of the following degrees of modification:

(1) Some of the weld material should be drilled and ground away where high stresses occur because of improper weldment relations.

(2) In addition to (1), other areas can be improved by the insertion of appropriately shaped gussets to transfer load more effectively from one member to another.

(3) In addition to (1) and (2), the launcher should be disassembled so that access will be provided to weld-in some internal diaphragms at certain critical areas in the horizontal 20-inch-diameter pipe frame.

(4) It is believed that if it is found desirable to replace the 4130 blocks on any launcher, it is practicable and feasible to do so. An integral forging seems to offer merit. Structural welds in the frame that may be cracked can be replaced by a skip burn-gouge and reweld procedure. The joint will remain intact, but the old weld can be entirely replaced without disassembly of the joint or serious misalinements.

The question arises about the integrity of launchers that may have undetectable flaws in some weld areas. The defects that cause the problem are cracks from the back, slag inclusions, improper penetration and poor adhesion of the weld material in the first pass, cold laps, etc. These defects create the environment for the problem of crack propagation due to the notch-sensitivity effect. However, in reviewing factors that influence notch sensitivity, it is noted that several conditions are favorable in this instance that minimize their effects:

(1) The base material and the weld metal in these launchers would generally be classified as ductile rather than brittle. A failure in ductile material caused by slowly applied loads is usually accompanied by yielding rather than a brittle failure.

(2) Stress relieving of the launcher frames would avoid the addition of residual stresses to those caused by any stress riser condition.

(3) The magnitude of downward loads on the launcher is greater by a ratio of 2 than the upward load. Correspondingly, the stresses arising from these loads have opposite signs and the same ratio of magnitude.

There is considerable evidence indicating that the damaging effect of a stress concentration in such a repeated cycle of stress is associated only with the magnitude of the completely reversed component of the stress cycle and not with the maximum stress in the cycle.

The blocks which support the pin that fastens the lower end of the release cylinders to the launcher end frame are welded directly to tubular members of the end frame and indirectly to two 1-inch-thick plates, which are welded to tubular members of the frame. These so-called indirect welds are highly stressed. Some yielding occurred in them. No cracking occurred, however, during any part of this test. The so-called direct welds are, for the most part, inaccessible or hidden. Their stress conditions for this test were unknown. The design calculations size the direct welds to take the entire load, neglecting the presence of the indirect welds. To modify this detail would be difficult as well as expensive. The static stability of the vehicle depends altogether on the integrity of this detail. As long as operating conditions and limitations remain as they are at this date, there is no need for any redesign or major modification; however, it is important to be aware of the potential hazard and to have a vigilant inspection attitude toward these welds. It is recommended that all exposed welds on these blocks be ground and polished to provide a surface on which the dye-penetrant test will have more sensitivity, thereby enabling detection of a crack early in its origin. These polished surfaces should never be painted, but should be covered with a rubber tape or glue that can be stripped off at any time. There is no necessity for any other precaution at this time if it is assumed that the launcher is proof tested with a reasonable size load, and that dye-penetrant inspections are conducted before and after each third launch. Better knowledge of the highly stressed welds has been obtained, and, therefore, these welds should be redefined before any subsequent dye-penetrant tests are performed.

## CONCLUDING REMARKS

As a result of the load tests made on a research and development Atlas launcher, the following conclusions were drawn:

1. The cracks that were known to exist before loads were applied did not grow a detectable amount because of the static or cyclic load applications.

2. High stresses occurred in the structural frame only in localized load transition areas.

3. The subject of repair, including rework of cracked welds and launcher modification to increase load capability, was given attention during the time interval of these tests. It has been determined that various degrees of repair, consistent with requirements, would be reasonable.

## APPENDIX

## SURFACE FORMING TECHNIQUES

The following procedure is used to apply the photoelastic coating to

(1) Liquid plastic (type PL-1) is mixed with a hardener and cast onto a leveled flat plate coated with a releasing agent. A 10 by 10 by 0.10 inch silicone rubber frame limits the flat area to be filled with liquid and determines the size and thickness of the sheet obtained.

(2) After 2 1/2 hours, when the plastic is in a semi-polymerized state (rubbery), the plastic sheet is lifted from the plate and molded to the shape of the area to be coated.

(3) After the various sheets have been cured, they are individually lifted from their respective areas, cleaned, and a bonding cement is applied to the contact surfaces. The sheets are then carefully and firmly placed back onto their respective areas to set, which takes about 12 hours at ambient temperature.

## REFERENCE

1. Baker, J. H.; and Buchy, P.: Stress Analysis - Centaur R & D Launcher. Rep. No. GDA63-1275, General Dynamics/Astronautics (Contract NAS3-3232), Jan. 29, 1964.

TABLE I. - DIFFERENCE OF PRINCIPAL STRAINS OBTAINED

FROM STATIC LOAD TESTS ON HOLDDOWN HEAD

| Point | Load, kips | | | | | | Remarks |
|---|---|---|---|---|---|---|---|
| | 192 up | 160 down | 232 up | 186 down | 232 down | 266 up | |
| | Difference of principal strains[a], $\epsilon_x - \epsilon_y$, μin./in. | | | | | | |
| 12 | 500 | -500 | 680 | -600 | -650 | 700 | Point 13 is used to illustrate stresses in tubular member away from the welded joint |
| 14 | -1100 | 800 | -1200 | 850 | 1200 | -1500 | |
| 13 | ---- | ---- | ---- | -340 | -410 | 560 | |
| 2 | 500 | ---- | 700 | -450 | ---- | ---- | |
| 31 | -1080 | 970 | -1180 | ---- | 1300 | -1300 | Point 32 is used to illustrate stresses in flat member in areas away from the weld |
| 32 | ---- | 550 | -580 | 590 | 690 | ---- | |
| [b]33 | -2480 | 1950 | -3400 | 3000 | 4000 | -4750 | |
| [b]43 | -2700 | ---- | -2920 | 2900 | 3600 | -3100 | |
| [b]47 | -3000 | 2480 | -3500 | 3300 | 4700 | -4900 | |
| [b]61 | 3800 | -3400 | 4100 | -3900 | -4500 | 6700 | Points 66 and 69 are not located on the edges and illustrate the strains in the weld |
| [b]65 | 3450 | -3000 | 4300 | -3350 | ---- | 6100 | |
| 66 | 2180 | -1950 | 2900 | -3000 | ---- | 3800 | |
| [b]67 | 1560 | -1400 | 2180 | -1560 | -2920 | 2480 | |
| 69 | | 1080 | -1400 | 1300 | 1550 | -1830 | |
| [b]6-10 | -3560 | 3020 | -4700 | 3400 | 4430 | -5960 | |
| 7 | ---- | ---- | ---- | ---- | 1680 | -1940 | The direction of principal strains is at 40° to the plane of symmetry |
| [b]81 | 2560 | -2400 | 2960 | -3600 | -4500 | 3350 | |
| 82 | 1350 | -1270 | 1850 | -1460 | -1720 | 2000 | |
| 86 | 1330 | ---- | 1510 | -1190 | -1600 | 1840 | |

[a]X-direction is perpendicular to the weld, Y-direction is parallel to it.

[b]Residual deformation (yielding) was observed.

TABLE II. - LOAD CYCLE FOR 50 ALTERNATE LOADINGS

| END FRAME | |
|---|---|
| QUADRANTS I AND IV | QUADRANTS II AND III |
| Load,[a] kips | |
| 64 up 196 down | 70 up 214 down |
| Check agent | |
| Photoelastic coating viewed in polarized light | Dye penetrant in accord with MIL-I-6866 |
| Test sequence | |
| First | Second |

TABLE III. - REDUCED STRAIN-GAGE DATA RESULTING FROM STATIC LOADS ON HOLDDOWN PIN

| Gage | Load,[a] kips | | | | | | Computed (266-kip load) | |
|---|---|---|---|---|---|---|---|---|
| | 192 up | 160 down | 232 up | 186 down | 232 down | 266 up | Moment (in.)(kips) | Direct load, kips |
| | Stress,[b] ksi | | | | | | | |
| 1 | 6.15 t | 10.2 c | 12.75 t | 12.3 c | 14.10 c | 17.7 t | 454 | 331 t |
| 2 | 1.05 t | 2.4 c | 3.6 t | 2.7 c | 3.0 c | 4.05 t | | |
| 3 | .9 c | 1.35 t | 2.25 c | 1.8 t | 2.1 t | 2.4 c | 25 | 65 c |
| 4 | 1.35 c | 2.4 t | 3.3 c | 2.7 t | 3.6 t | 3.75 c | | |
| 5 | 1.05 c | 1.65 t | 3.0 c | 2.4 t | 3.0 t | 3.45 c | 350 | 266 c |
| 6 | 5.1 c | 7.5 t | 12.3 c | 9.3 t | 11.7 t | 13.97 c | | |
| 7 | 6.3 t | 9.0 c | 15.3 t | 11.25 c | 12.9 c | 16.5 t | 736 | 66 c |
| 8 | 8.25 c | 13.2 t | 19.8 c | 16.35 t | 20.2 t | 22.7 c | | |
| 9 | 1.2 c | 1.5 t | 2.25 c | 2.4 t | 2.84 t | 3.46 c | Section properties unknown | |
| 10 | 1.05 c | 2.4 t | 2.7 c | 2.4 t | 3.75 t | 4.8 c | | |
| 11 | 2.7 t | 4.65 c | 7.5 t | 5.7 c | 6.45 c | 8.4 t | 268 | 27 t |
| 12 | 1.95 c | 3.3 t | 4.95 c | 3.45 t | 5.4 t | 5.85 c | | |

[a]Load applied to the main holddown release pin.

[b]Tensile stress indicated by t; compressive stress indicated by c.

TABLE IV. - PRINCIPAL STRAINS OBTAINED FROM 128-KIP STATIC LOAD ON STABILIZING PIN

| Point | Difference of principal strains, $\epsilon_x - \epsilon_y$, μin./in. |
|---|---|
| $A_L$ | -2050 |
| $A_R$ | -1840 |
| $B_L$ | -1730 |
| $B_R$ | -760 |
| $C_L$ | 1940 |
| $C_R$ | 1900 |

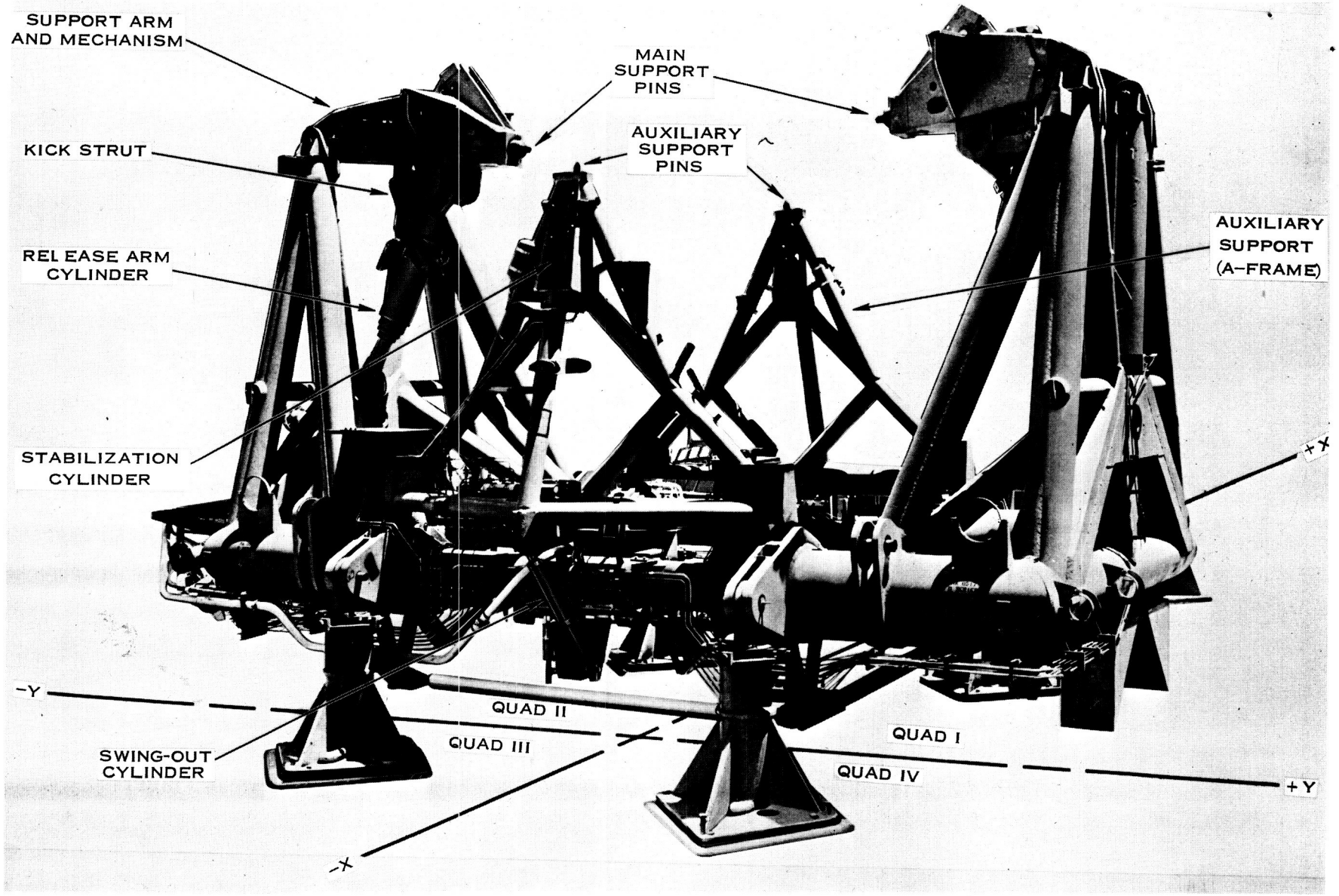


Figure 1. - Vehicle launcher configuration.

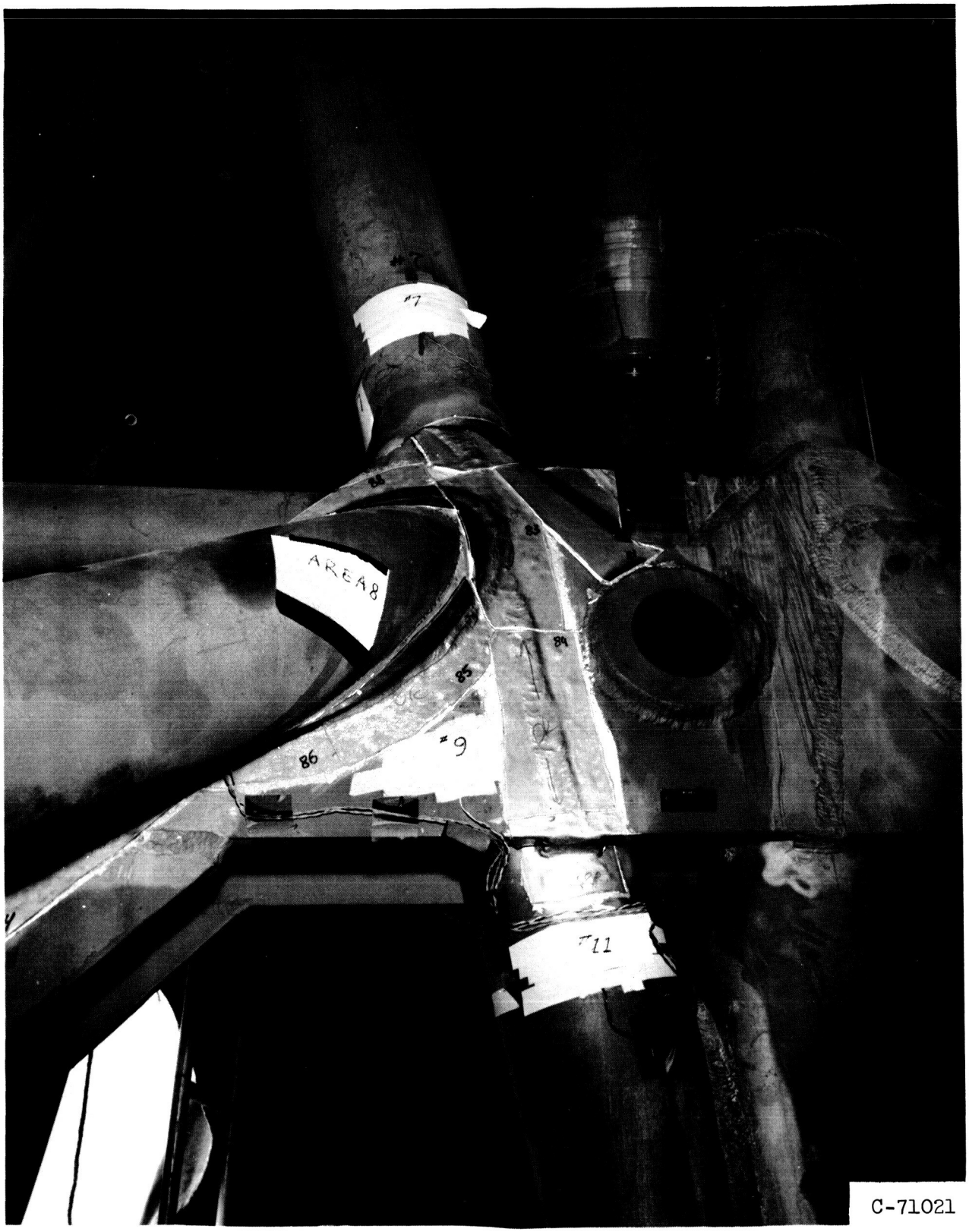


Figure 2. - Inside view of trunnion support area in quadrants I and IV showing strain gages 7, 9, and 11.

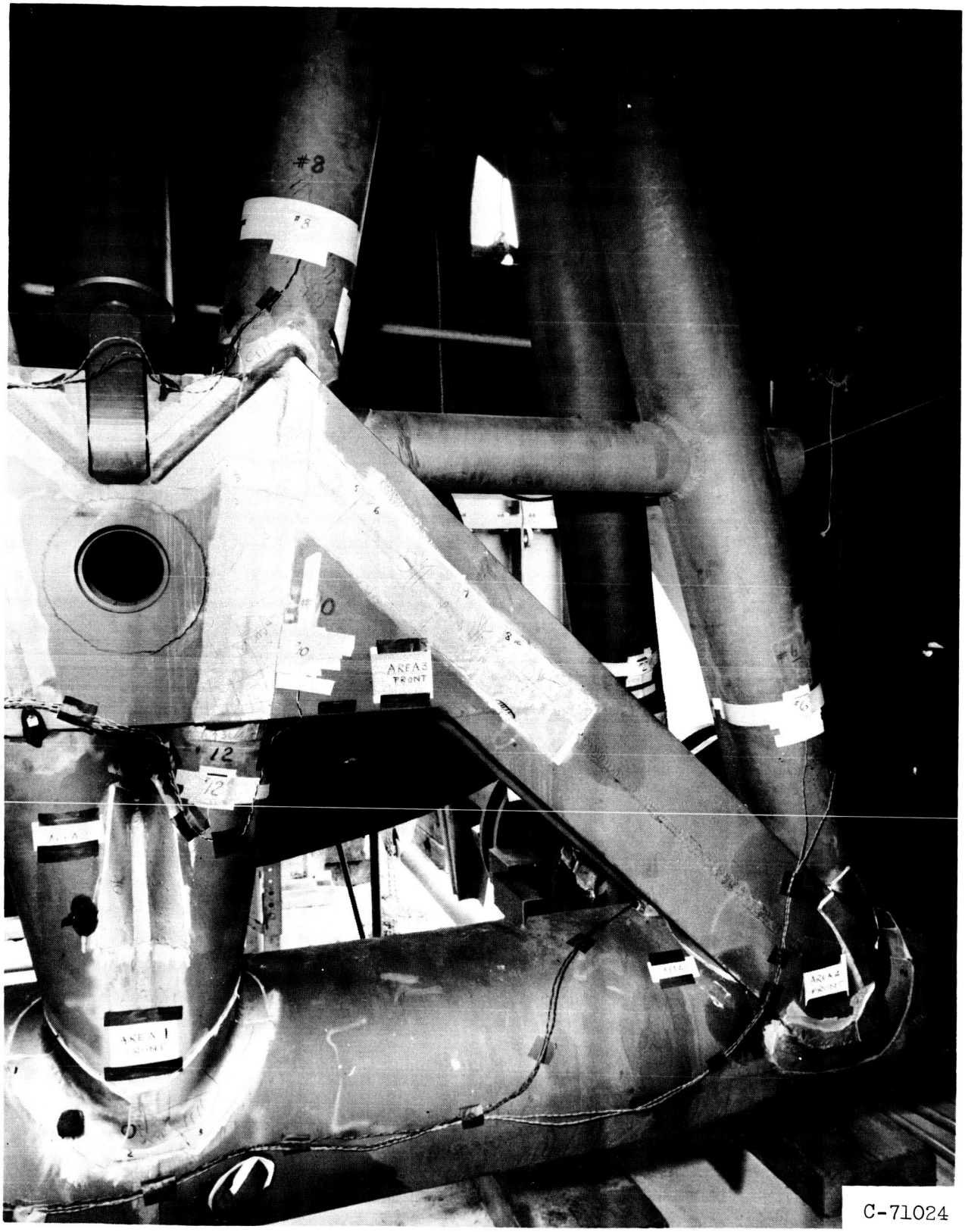


Figure 3. - Outside view of end frame in quadrant I showing strain gages 6, 8, 10, and 12.


Figure 4. - Outside view of diagonal bracing members of horizontal frame joint in quadrant I showing strain gages 2 and 4.

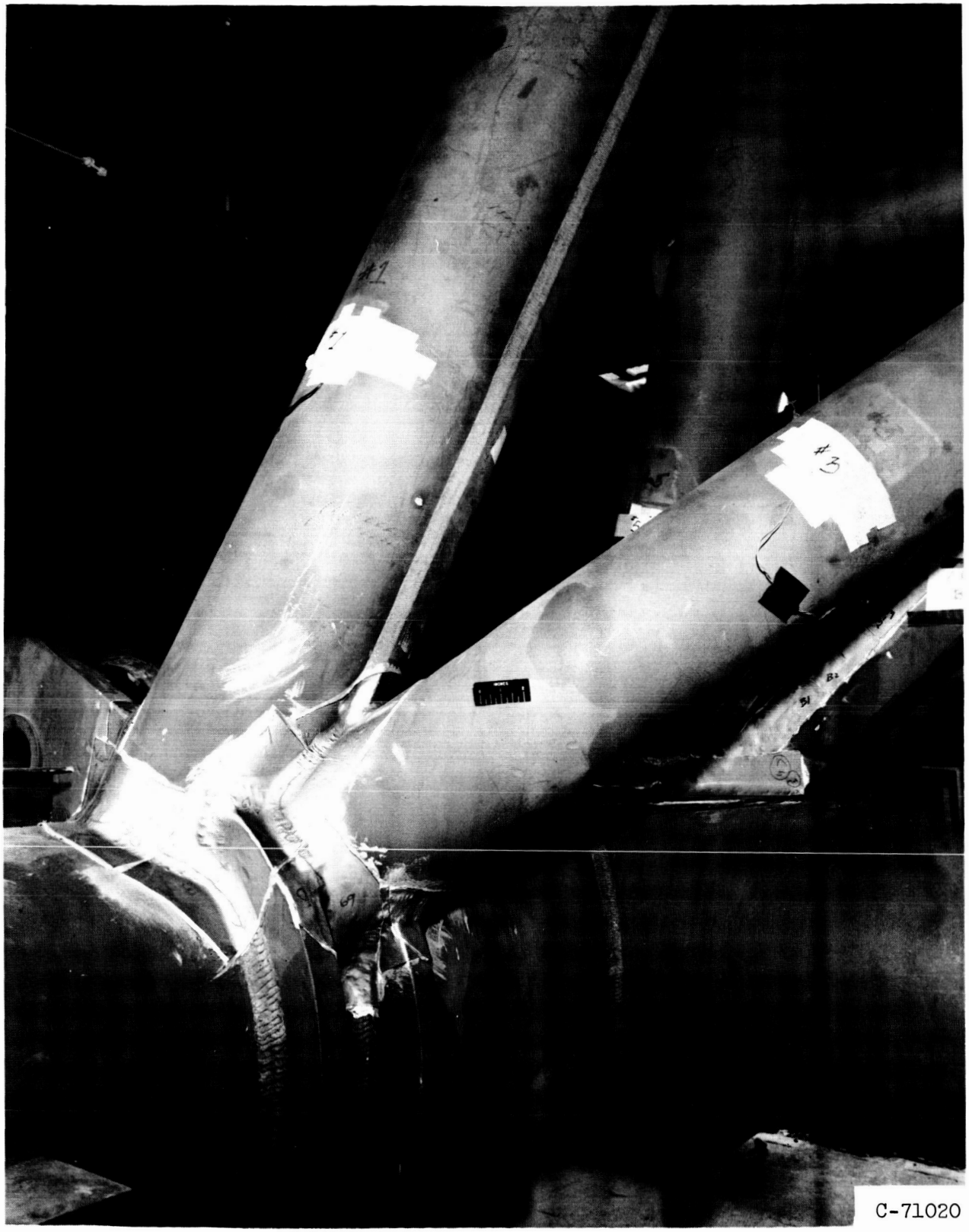


Figure 5. - Inside view of diagonal bracing members of horizontal frame joint in quadrant I showing strain gages 1 and 3.


Figure 6. - Inside view of corner post horizontal frame joint in quadrant I showing strain gage 5.

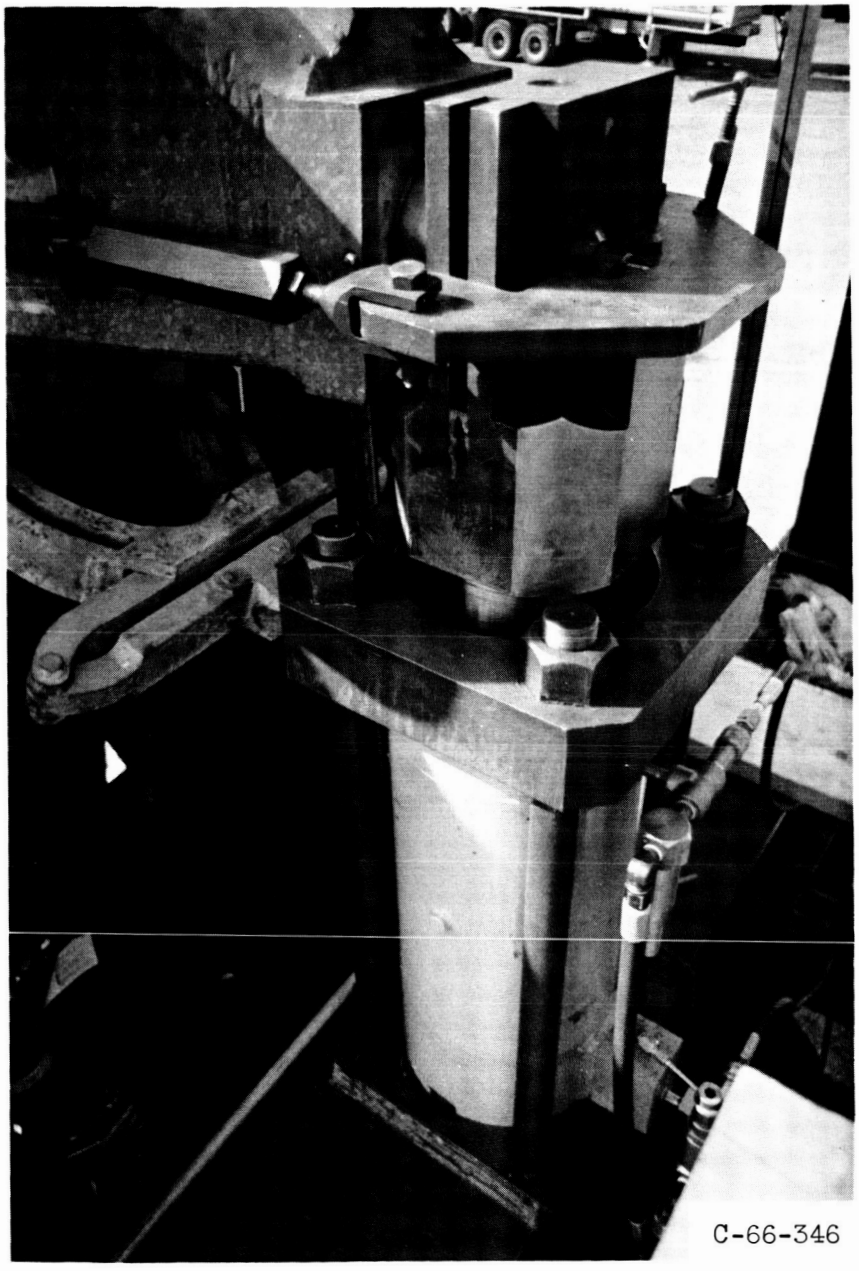


Figure 7. - Cylinder main release pin engagement.

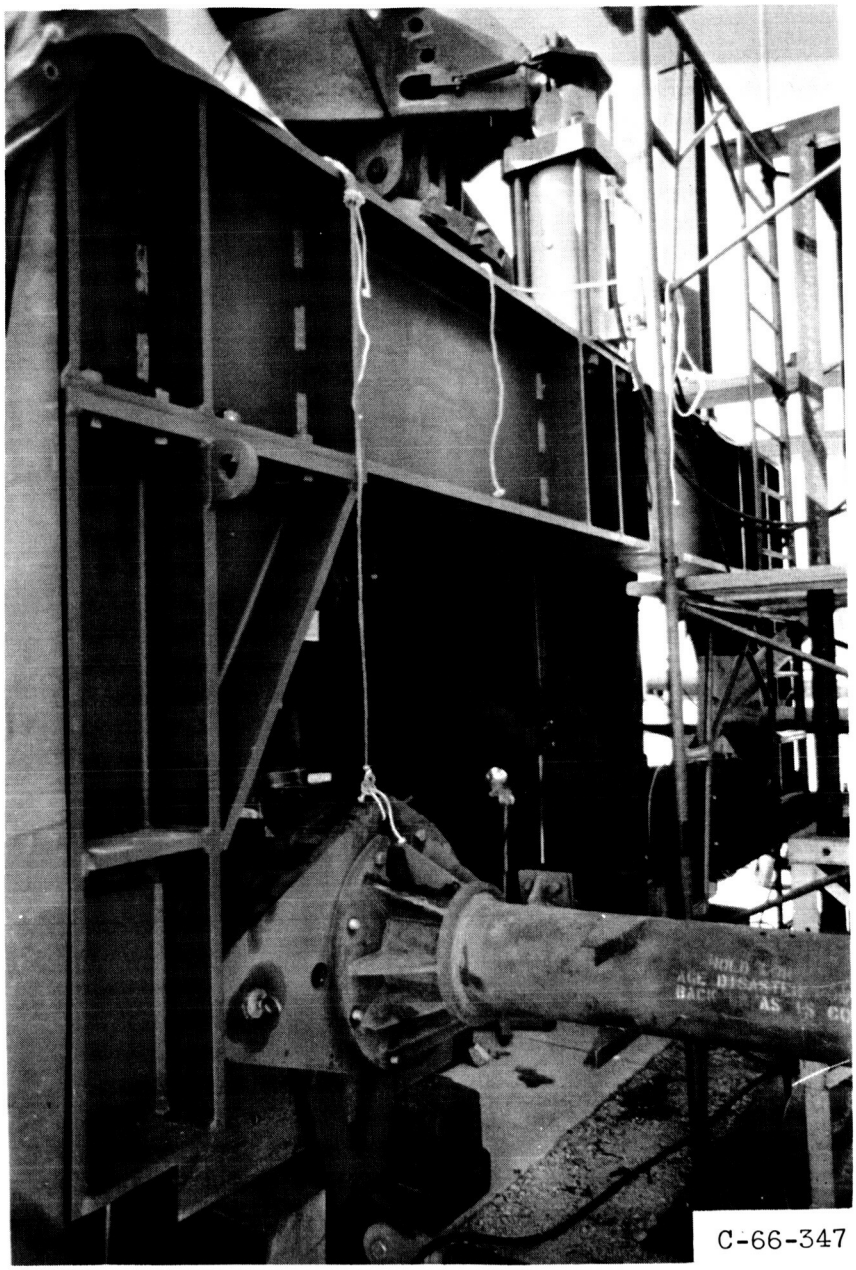


Figure 8. - Test fixture.


Figure 9. - Arrangement for measuring vertical deflection.

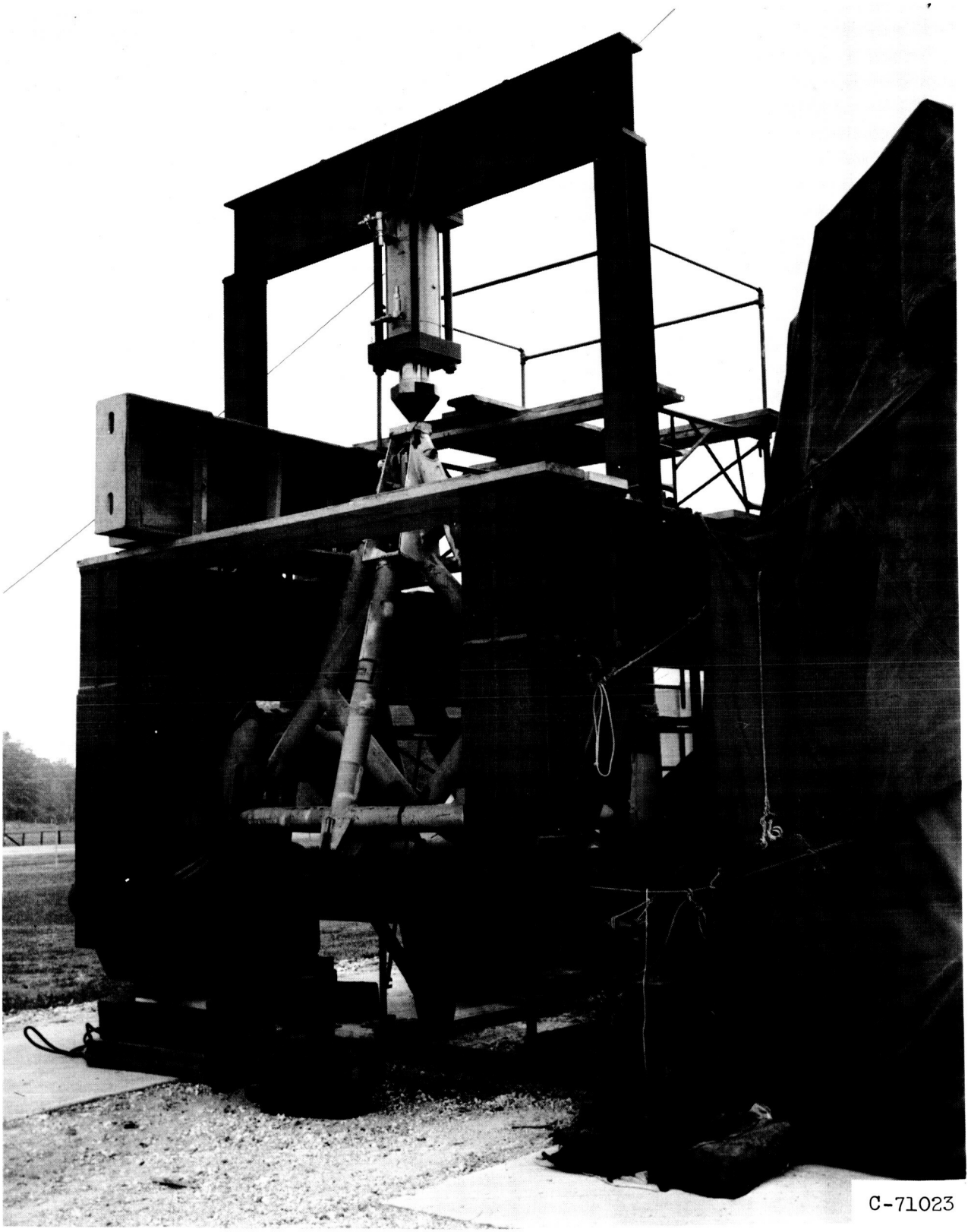


Figure 10. - Setup for balance longeron frame test.

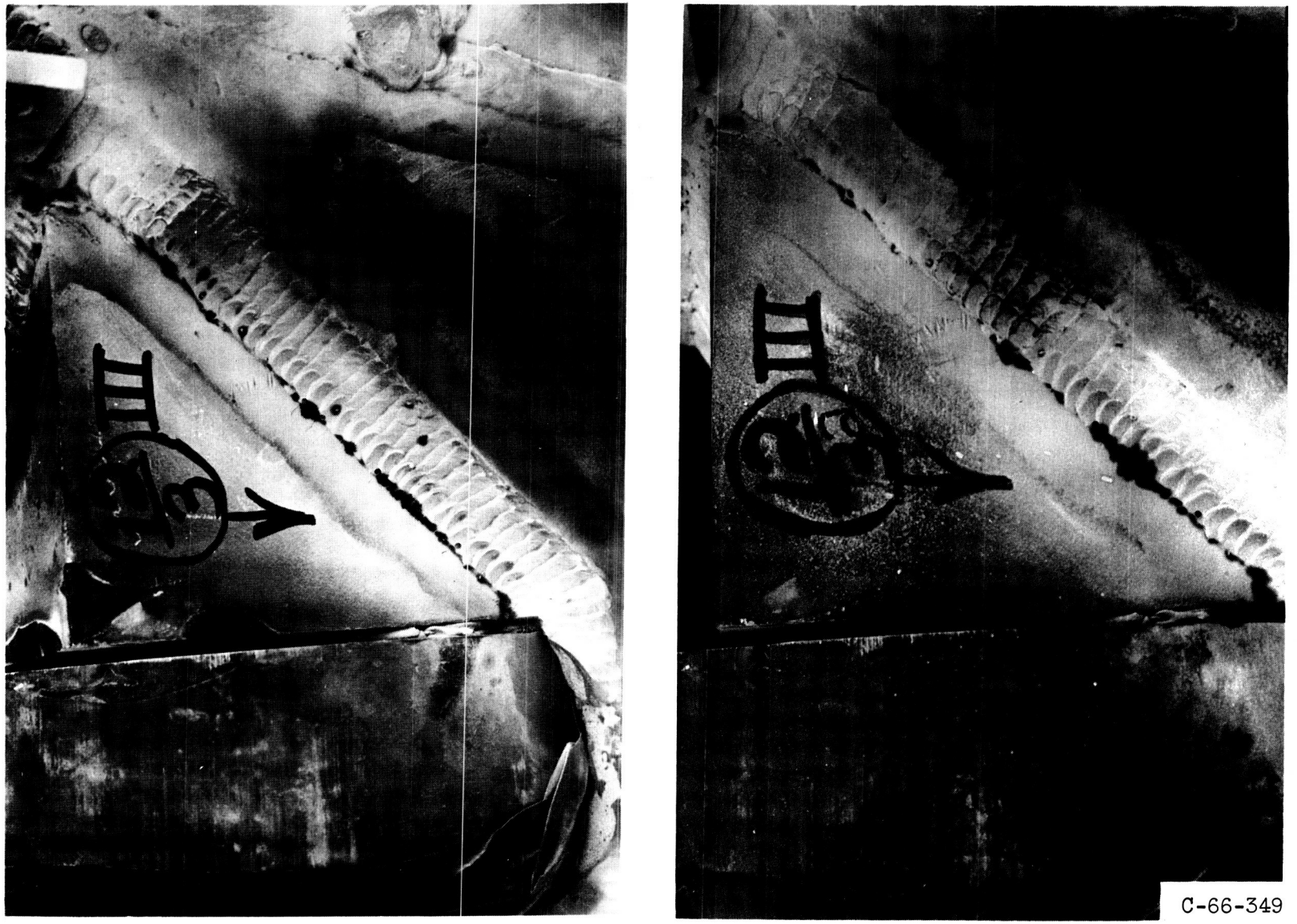


(a) Before loading in area 12.

(b) After loading in area 12.

Figure 11. - Dye-penetration indication before and after cyclic loading in quadrant III.

(c) Before loading in area 7.


(d) After loading in area 7.

Figure 11. - Continued.

(e) Before loading in area 5.

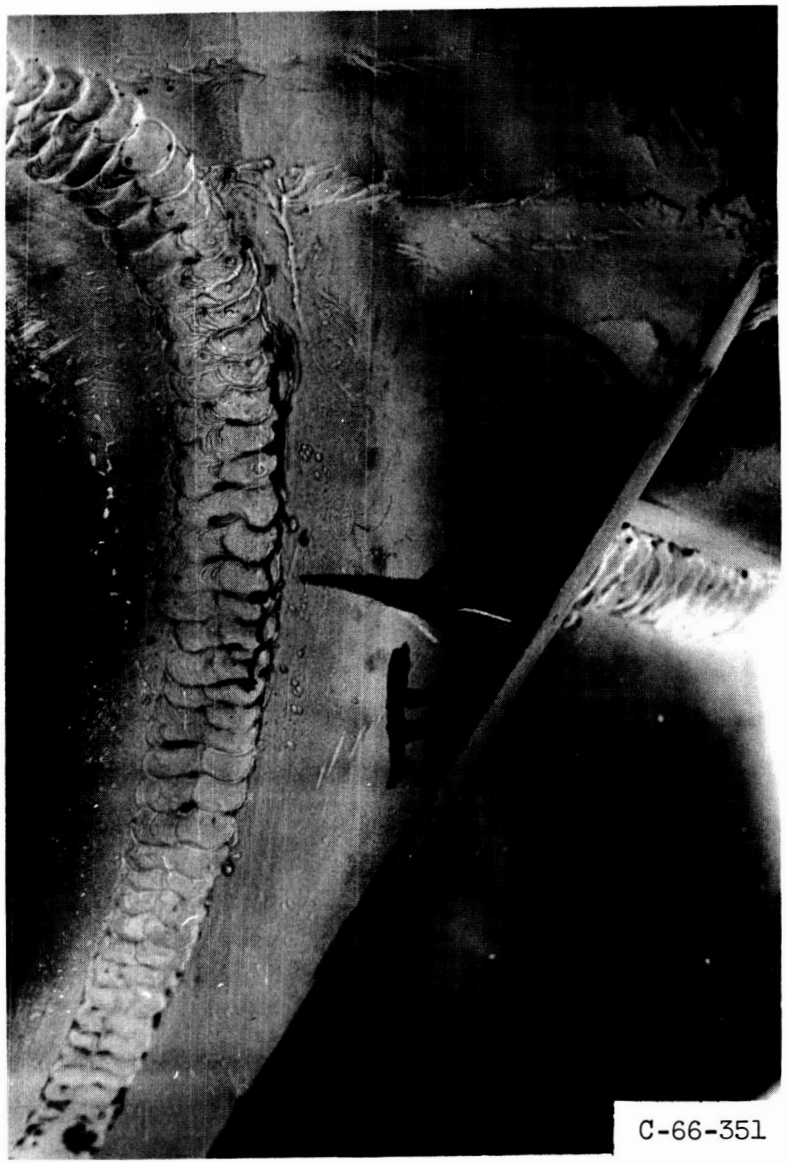


(f) After loading in area 5.

Figure 11. - Concluded.

| Point | Ultimate tensile strength, $F_{tu}$, ksi | Point | Ultimate tensile strength, $F_{tu}$, ksi |
|---|---|---|---|
| 1III | 59 | 7III | 69 |
| 2II | 75 | 8II | 74 |
| 3II | 77 | 9II | 77 |
| 4II | 71 | [a]10 | 78 |
| 5III | 75 | 11III | 92 |
| 6III | 85 | 12III | 62 |

[a]Location unknown.

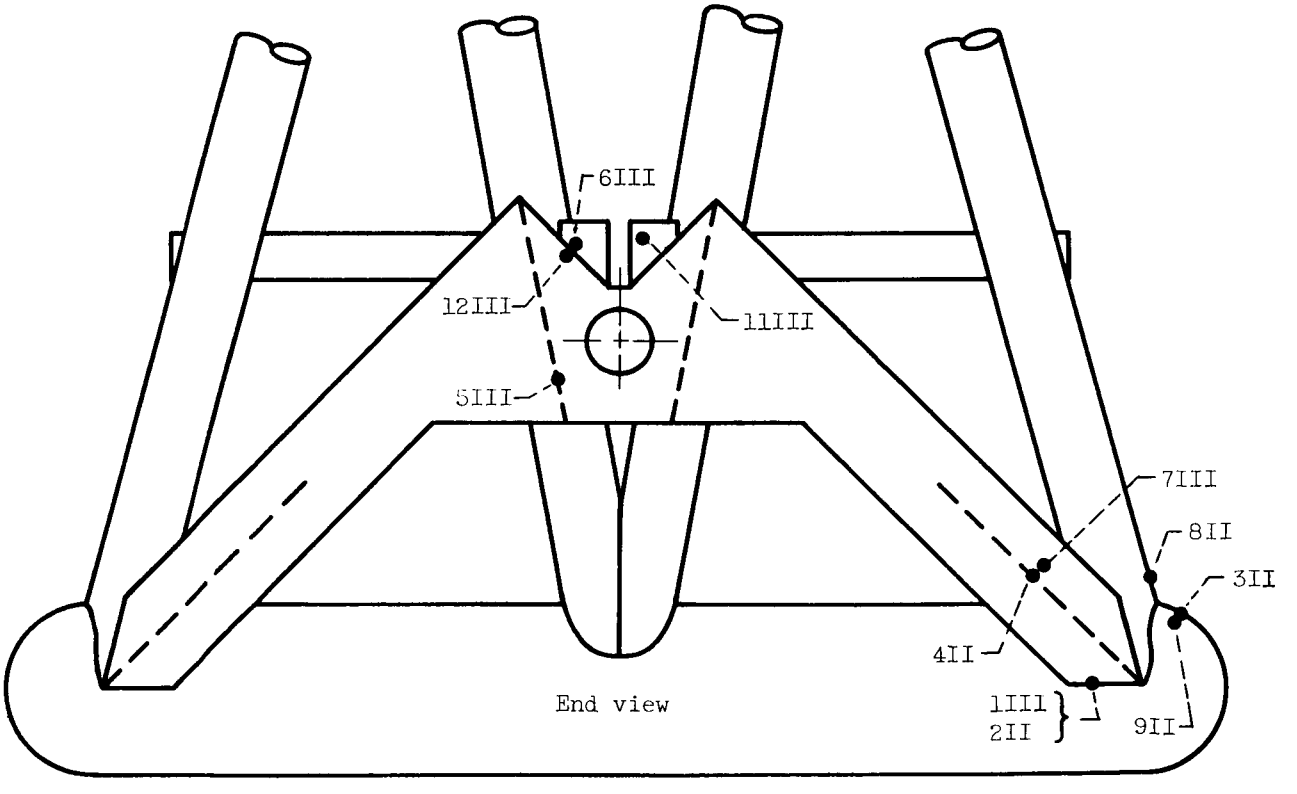


Figure 12. - Point nomenclature example: 3II is point 3 located in quadrant II. (Points 1 to 6 are in weld material, whereas points 7 to 12 are in base metal.)

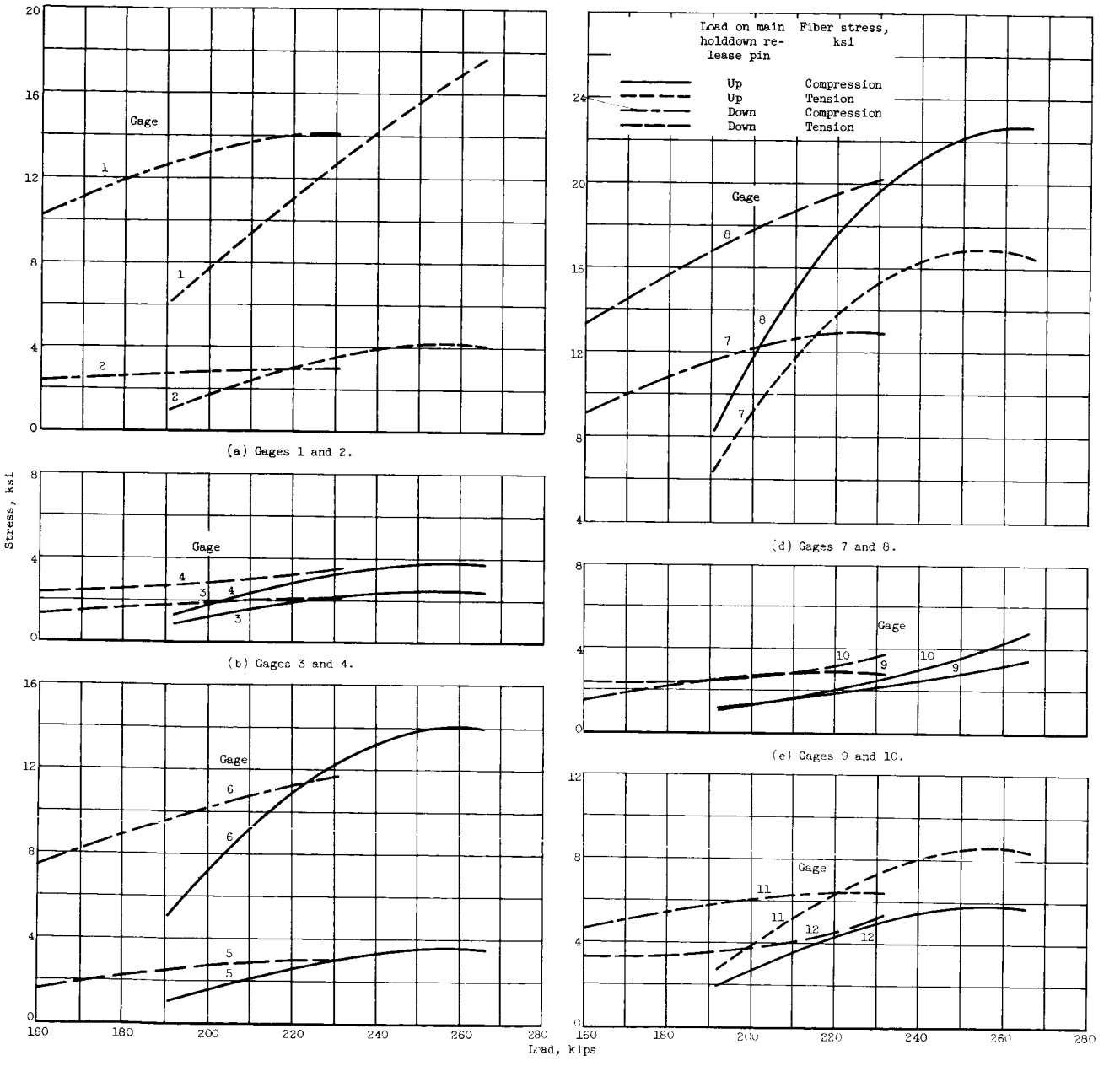


(a) Gages 1 and 2.

(b) Gages 3 and 4.

(c) Gages 5 and 6.

(d) Gages 7 and 8.

(e) Gages 9 and 10.

(f) Gages 11 and 12.

Figure 13. - Reduced strain-gage data resulting from static loads on holddown pin (see table III).

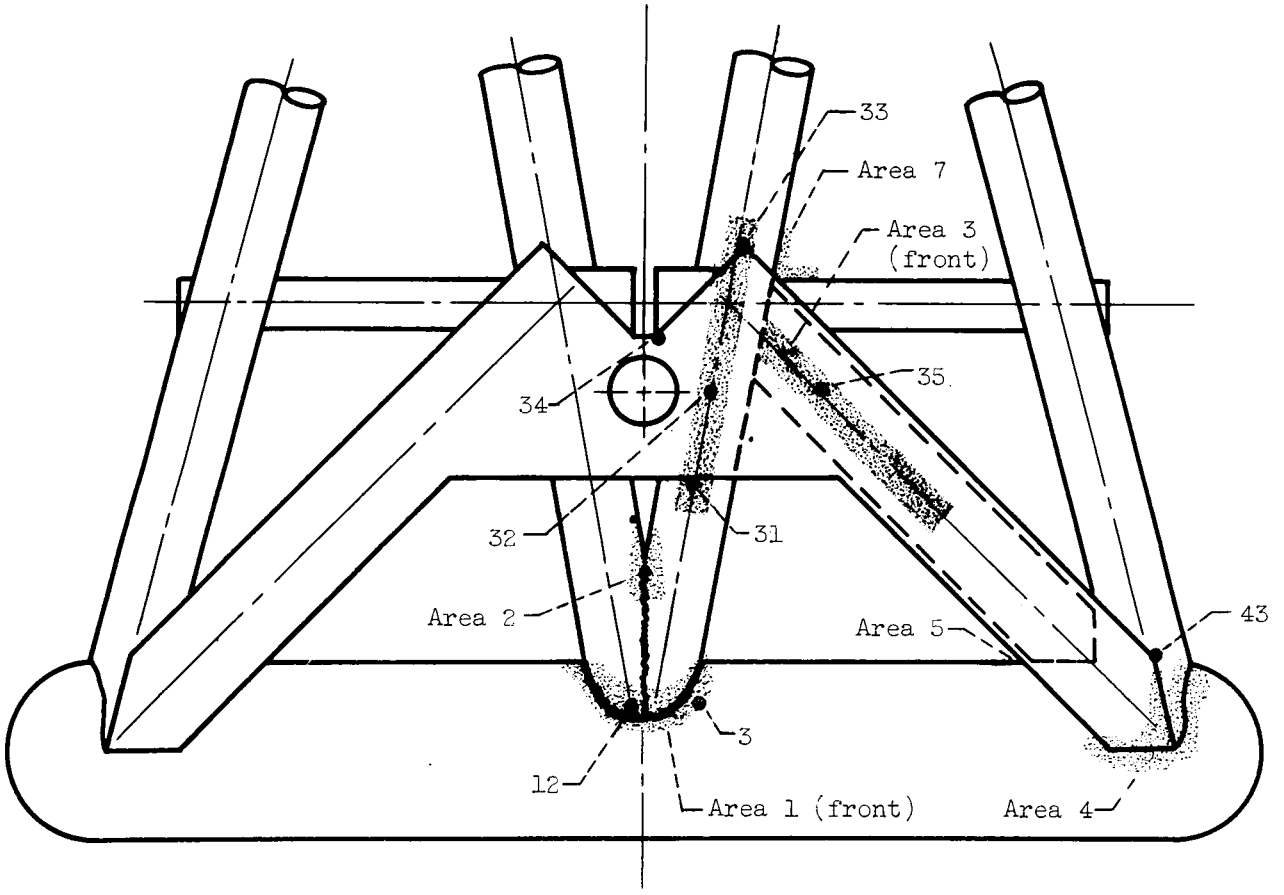


Figure 14. - Outside view of end frame in quadrants IV and I showing photoelastic application areas.

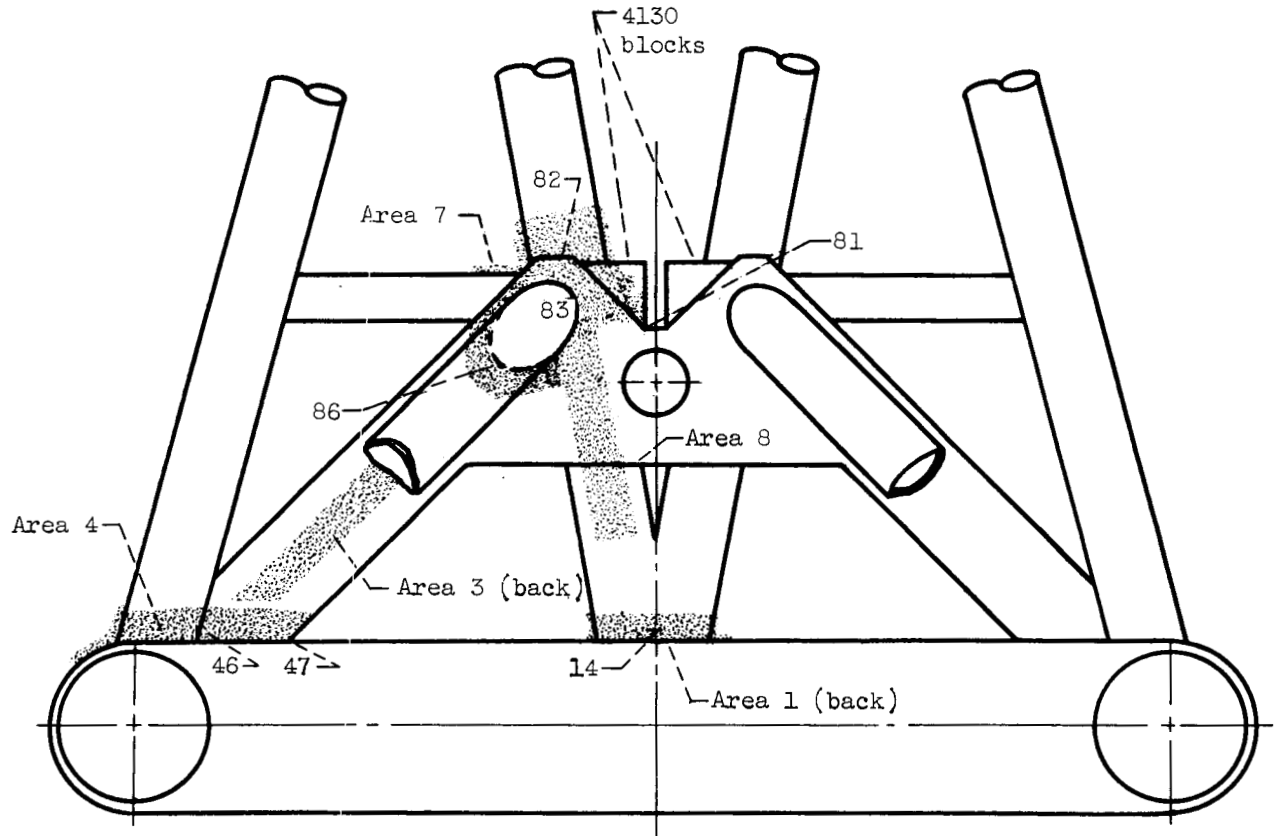


Figure 15. - Inside view of end frame in quadrants I and IV showing photoelastic application areas.

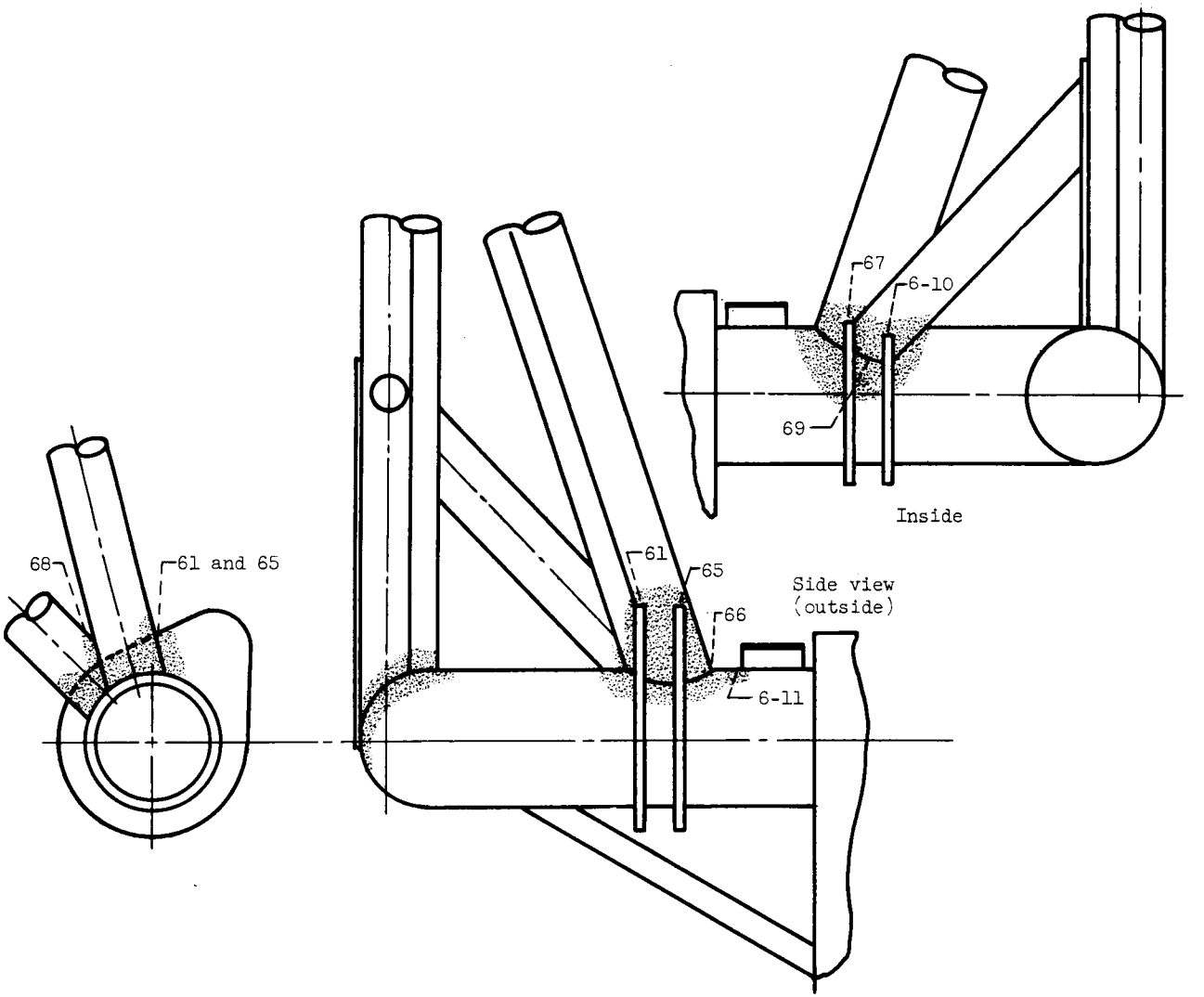


Figure 16. - Inside and outside views of end frame in quadrant I showing photoelastic application areas.

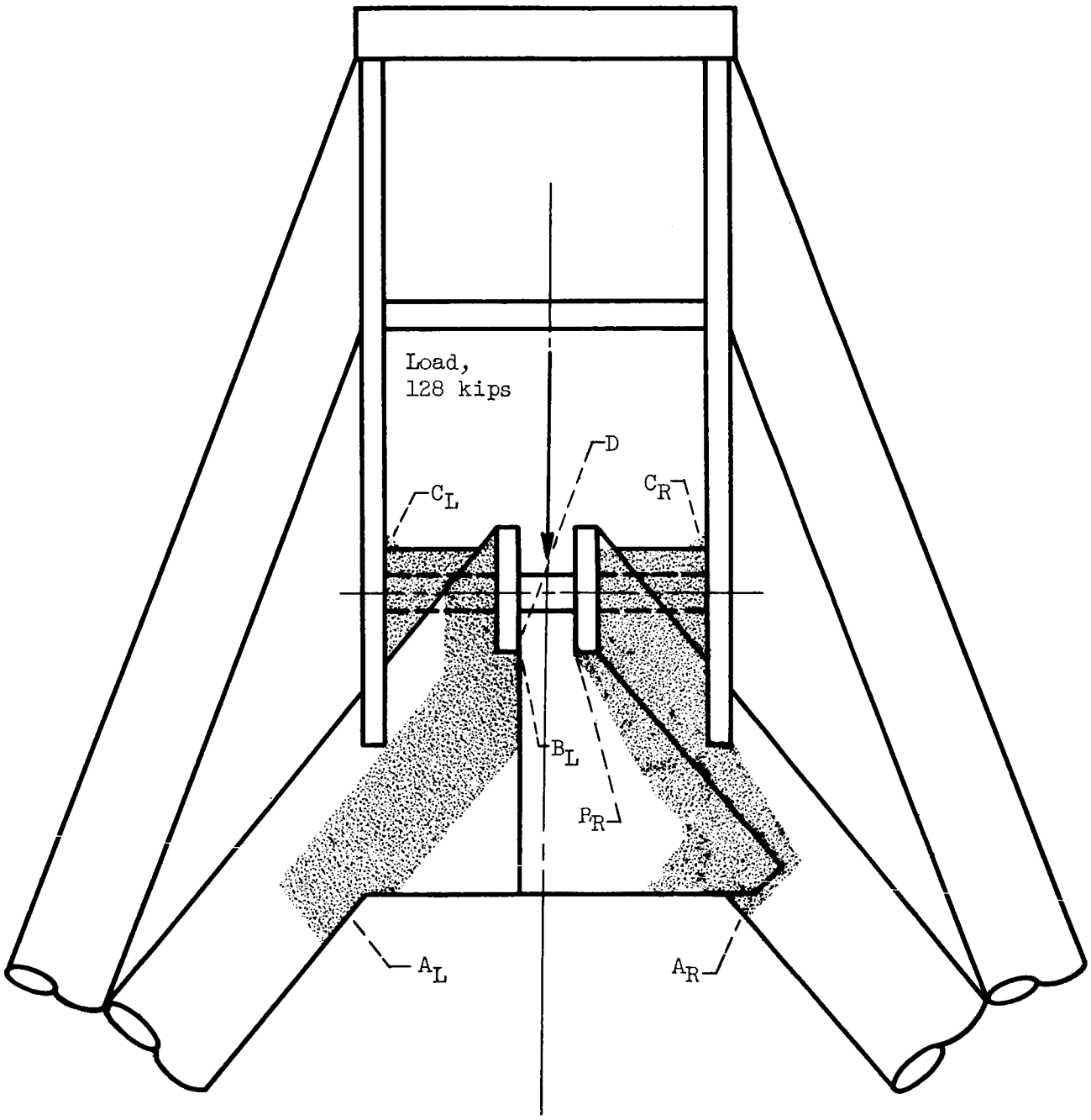


Figure 17. - Inside view of top of auxiliary frame showing load and photoelastic application area.